Alterations in *CDH15* and *KIRREL3* in Patients with Mild to Severe Intellectual Disability

Kavita Bhalla,[1,4,5] Yue Luo,[1,4] Tim Buchan,[2] Michael A. Beachem,[1] Gregory F. Guzauskas,[1] Sydney Ladd,[1] Shelly J. Bratcher,[1] Richard J. Schroer,[1] Janne Balsamo,[2] Barbara R. DuPont,[1,3] Jack Lilien,[2] and Anand K. Srivastava[1,3,*]

Cell-adhesion molecules play critical roles in brain development, as well as maintaining synaptic structure, function, and plasticity. Here we have found the disruption of two genes encoding putative cell-adhesion molecules, *CDH15* (cadherin superfamily) and *KIRREL3* (immunoglobulin superfamily), by a chromosomal translocation t(11;16) in a female patient with intellectual disability (ID). We screened coding regions of these two genes in a cohort of patients with ID and controls and identified four nonsynonymous *CDH15* variants and three nonsynonymous *KIRREL3* variants that appear rare and unique to ID. These variations altered highly conserved residues and were absent in more than 600 unrelated patients with ID and 800 control individuals. Furthermore, in vivo expression studies showed that three of the CDH15 variations adversely altered its ability to mediate cell-cell adhesion. We also show that in neuronal cells, human KIRREL3 colocalizes and interacts with the synaptic scaffolding protein, CASK, recently implicated in X-linked brain malformation and ID. Taken together, our data suggest that alterations in CDH15 and KIRREL3, either alone or in combination with other factors, could play a role in phenotypic expression of ID in some patients.

Introduction

Intellectual disability (ID), also known as intellectual and developmental disability or mental retardation, is the most frequently reported developmental disability, affecting cognitive function in about 1%–3% of people worldwide. Intellectual disability, often diagnosed as developmental delay in early childhood, is a genetically and clinically heterogeneous condition characterized by below-average intellectual functioning (IQ < 70) in conjunction with significant limitations in adaptive functioning.[1] The causation in at least half of all ID cases is still unknown.[2,3] Among the identifiable genetic causes, chromosome abnormalities, single-gene mutations, and multifactorial interactions account for approximately 30% of ID overall. It is expected that the genetic component of ID, in part, is due to alterations in molecular pathways involved in cognitive function.[2,4]

A large number of genes distributed throughout the genome are anticipated to cause ID. This is well established for the X chromosome, where more than 80 genes that cause syndromal and nonsyndromal ID have been identified.[3–5] Compared with genes on the X chromosome, very few autosomal genes have been implicated in ID. The autosomal ID genes identified are primarily involved in syndromal and metabolic conditions and only five are involved in nonsyndromal ID.[6–12] Only a few families or unrelated individuals with autosomal-recessive ID have been found to have mutations in these genes.[6]

Identification of autosomal genes associated with ID has proven very difficult primarily because of the lack of large families for linkage analysis.[3] Furthermore, finding ID-causing gene mutations in candidate genes has been difficult because of the enormous genetic heterogeneity and rarity of mutations in any individual gene in the ID population. It has been observed that mutations in most cloned X-linked ID genes have a very low ($<1.0\%$) prevalence in patients with ID.[5] However, a significant contribution of both common and rare gene variants in disease phenotypes has been suggested in several recent studies.[13–15]

Growing evidence indicates that defects in synapse formation or synaptic plasticity are major causes of ID.[4,16] Cell-adhesion molecules of the cadherin and immunoglobulin (Ig) superfamilies play critical roles in brain development, as well as maintaining synaptic structure, function, and plasticity.[17] In this study, we characterized a balanced translocation in a female patient with severe ID that truncates two genes encoding such cell-adhesion molecules, *CDH15* (cadherin superfamily) (MIM 114019) and *KIRREL3* (Ig superfamily) (MIM 607761). These findings prompted us to analyze a large cohort of patients with ID of unknown cause for alterations in the two genes. We identified and characterized seven variations in key functional domains of CDH15 and KIRREL3 in unrelated patients with ID. We show that rare variants of CDH15 are functionally significant. We also show that in neuronal cells, KIRREL3 interacts with the synaptic scaffold protein calmodulin-associated serine/threonin kinase (CASK) (MIM 300172), recently implicated in X-linked brain abnormalities and ID.[18–20] Consistent with a predicted role of KIRREL3-CASK in brain function, a role for mouse Kirrel3 in synaptogenesis has been suggested[21] and the

[1]J.C. Self Research Institute of Human Genetics, Greenwood Genetic Center, 113 Gregor Mendel Circle, Greenwood, SC 29646, USA; [2]Department of Biological Sciences, University of Iowa, Iowa City, IA 52242, USA; [3]Department of Genetics & Biochemistry, Clemson University, Clemson, SC 29634, USA
[4]These authors contributed equally to this work
[5]Present address: Division of Endocrinology, Diabetes & Nutrition, University of Maryland, Baltimore, MD 21201, USA
*Correspondence: anand@ggc.org
DOI 10.1016/j.ajhg.2008.10.020.

deletion of Cask in mice have been shown to impair synaptic function.[22]

Material and Methods

Patients and Control Samples

CMS3377 is a 56-year-old white female with severe ID (with an intelligence quotient of 16). She began walking at about 3 years of age. Physical examination revealed her head circumference to be 54.5 cm (45th centile). She had alternating exotropia, flat midface, some downslanting of the lower eyelids, a thin nasal bridge, a rounded nasal tip, a nasal septum below the alae nasi, and small chin. Other clinical features included short fifth fingers and fingernails, broad and short feet with short toes, and 2-3-4 syndactyly on the right and 2-3 syndactyly on the left. Routine high-resolution chromosome analysis on blood revealed an apparently balanced translocation t(11;16)(q24.2;q24). Furthermore, no additional obvious chromosomal rearrangements at or near the chromosomal breakpoints or unrelated to the translocations were detected by array-CGH analyses via a targeted GenoSensor Array 300 and the Human Mapping 250K (NSP) array. No karyotype information was available from the parents, who are deceased but apparently normal phenotypically.

Mutation screening was performed in a cohort of 657 unrelated patients with ID of unknown etiology. These patients were negative for the *FMR1* (MIM 309550) expansion. Control samples consisted of 800 normal individuals. The study was approved by the Institutional Review Board of the Self Regional Healthcare and the National Institutes of Health Office of Human Research Protection.

FISH Analysis

BAC and PAC DNAs were isolated with QIAGEN Mini-Prep columns and were labeled by incorporation of biotin-11-dUTP (Sigma) or digoxigenin-11-dUTP (Boehringer Mannheim) by nick translation with DNA polymerase I (Life Technologies). Metaphase chromosome spreads were obtained from lymphoblastoid cell lines from patients and FISH was performed as described previously.[23] Chromosome-specific labeled centromeric alphoid probes were used for chromosome 11 and 16 identification. The labeled probes were visualized with FITC-avidin (for Biotin) or rhodamine-labeled anti-digoxigenin and the chromosomes were counterstained with DAPI. Images were examined under a Zeiss Axiphot fluorescent microscope.

Inverse-PCR and Cloning of Junction Fragment

For inverse-PCR, genomic DNA from patient CMS3377 was digested with Pst1 and electrophoresed on a 0.8% Seakem LE agarose gel. DNA fragments between 1.0 and 1.1 kb were gel-purified with QIAquick gel extraction kit. Fragments were self-ligated at 14°C for 14 hr at a concentration of 3 ng/μl with 1 unit of T4 DNA ligase (Promega, Madison, WI) and amplified with *CDH15* exon 2/intron 2 complementary primers (2Fa and 2Ra; Table S1 available online), in order to amplify flanking sequences. The PCR reaction was performed on 1 μl of self-ligated fragments in a total volume of 30 μl, containing 10 μM of each primer, 25 μM dNTPs, 1× PCR buffer (1.5 mM $MgCl_2$), and 1 unit of Taq polymerase, under the following conditions: 95°C for 4 min, 35 cycles of 95°C for 30 s, 60°C for 30 s, and 72°C for 2 min, with a final extension of 7 min. A nested PCR was performed with primers 2Fa2 and 2Ra2 (Table S1) and PCR mix 1 as the template. The PCR product was gel-purified, subcloned, and sequenced.

Expression Analysis

Total RNA from Epstein-Barr virus (EBV)-transformed lymphoblastoid cell lines or lymphocytes was isolated with Trizol LS (Life Technologies) and first-strand synthesis was performed with SuperScript first-strand synthesis system for RT-PCR (Invitrogen). 4 μg of total RNA was mixed with 50 ng/μl of random hexamers supplied with the kit in a final volume of 10 μl with DEPC-treated sterile water. Standard PCR of the first strand cDNA was performed in a final volume of 10 μl with 0.5 units of Taq DNA polymerase (Sigma) with 0.02 μM of TaqStart antibody (Clontech), 10 μM of each primer, 250 μM of dNTPs, and 1× PCR buffer (1.5 mM $MgCl_2$). Typical PCR conditions were: initial denaturation at 95°C for 150 s followed by 30–40 cycles of 95°C for 30 s, 60°C–65°C for 30 s, and 72°C for 30–60 s with a final extention of 5 min. 1/10, 1 μl, and 2 μl of the cDNA was used for *ACSF3* and *ST3GAL4* (MIM 104240), *CDH15*, and *KIRREL3* genes, respectively, to carry out quantitative PCRs. Primers are listed in Table S1. Initially, the PCR was performed for various PCR cycles with random lymphoblastoid cDNA. The PCR was then carried out in a final volume of 30 μl. Different volumes of the amplified PCR products were analyzed on the 2% agarose gels with ethidium bromide staining in 1× TBE buffer. Having standardized the number of PCR cycles and volumes of the respective PCR product to be loaded on the agarose gel, the normal and patient cDNA were amplified with gene-specific primers. Quantitative analysis was performed with AlphaEase software supplied with the AlphaEase FC Imaging system (IS-2200, Alpha Innotech).

Mutation Screening

Mutations were analyzed with Incorporation PCR SSCP.[24] Amplicons were amplified in a 10 μl reaction volume containing 10–20 ng of genomic DNA, 1× PCR buffer (Sigma), 0.125 mM dNTPs, 1 μCi of [α-^{32}P]dCTP (3000 Ci/mmol), 0.50 μM of each primer (Table S1), and 1.0 unit of Taq polymerase with the following PCR conditions: initial denaturation at 95°C for 300 s, followed by 30 s at 95°C, 30 s at 55°C–68°C, and 60 s at 72°C for 30–35 cycles. ^{32}P-labeled PCR products were denatured for 3 min at 96°C in formamide/NaOH containing loading buffer and analyzed on 0.5× MDE (BioWhittaker Molecular Applications) gel run at 8 W for 17–20 hr at room temperature. The radioactive signal was visualized with X-Omat film (Eastman Kodak).

Both strands of PCR products from patients with abnormally migrating bands and a normal control were amplified and sequenced with DYEnamic ET Dye Terminator Cycle sequencing Kit (GE Healthcare) and an automated MegaBACE 1000 DNA Analysis system (GE Healthcare). Sequences were analyzed with the DNASTAR program (Madison WI).

Site-Directed Mutagenesis and Transfection

E. coli containing the plasmid pOTB7 with the *CDH15* insert were grown overnight and plasmid DNA was isolated with a QIAGEN Midiprep Kit and ethanol precipitation. Point mutations were introduced into the wild-type sequence with PCR site-directed mutagenesis. For each mutation, a forward and a reverse primer were designed containing a Kozak sequence, a start codon, and the desired mutation flanked on both sides by 14 bases homologous to wild-type *CDH15*. Purified PCR products were ligated into the phCMV3 (Gene Therapy Systems, San Diego, CA) at the 3′ position of the HA tag. DNA from all constructs was sequenced.

L-cells were grown in 60 mm dishes in Dulbecco's modified Eagle's medium (DMEM; Life Technologies Inc., Grand Island, NY)

with 10% FBS and 1% P/S, to 60% confluence. The medium was then changed to OptiMem (Life Technologies Inc.) and cells transfected with Lipofectamine (Life Technologies Inc.) according to the manufacturer's procedures. Stable clones were selected in culture medium containing 500 μg/ml G418.

Cell-Surface Labeling

L-cells expressing *CDH15* constructs were grown to confluence in 60 mm culture plates washed three times with ice-cold PBS (pH 8.0). The cell-membrane-impermeable reagent, NHS-LC-S-S-Biotin (Pierce, Rockford, IL), was then added to 0.5 mg/ml and incubated at 4°C for 30 min. Cells were washed three times with ice-cold PBS (pH 8.0) to remove any remaining biotinylation reagent and lysed in RIPA buffer (50 mM Tris [pH 7.4], 150 mM NaCl, 0.1% SDS, 0.0 5% DOC, 1% NP-40) containing a cocktail of protease inhibitors (Calbiochem, San Diego, CA) and 10 μg/ml DNase. The cleared lysates were then incubated with streptavidin-conjugated magnetic beads (Roche, Indianapolis, IN), and the beads were washed several times and eluted with SDS-sample buffer. Eluted material was analyzed by western blots with anti-HA antibody (Roche).

Cell Aggregation Assay

Cells grown to confluence in 60 mm plates were washed with HBSGKCa (25 mM HEPES [pH 7.2], 150 mM NaCl, 3 mM KCl, 2 mM glucose, and 1 mM $CaCl_2$) and released by incubation with 0.2% trypsin in the same buffer, for 3 min at room temperature. The cells were collected by centrifugation at 2000 × g and resuspended in DMEM/HEPES (pH 7.2) containing 5 μg/ml antipain and 10 μg/ml DNAase. About 10^3 cells were aliquoted in 35 mm plates, in 3 ml DMEM/HEPES and incubated at 37°C and 70 RPM. After 3 hr, cultures were examined under the microscope and photographed. The number of aggregates and single cells was counted in 6 separate aliquots containing ≈100 particles each.

KIRREL3 and CASK Expression Constructs

KIRREL3 (IMAGE clone 5195277) and *CASK* (IMAGE clone 40125862) cDNA clones were purchased from Open Biosystems (Huntsville, AL). The *KIRREL3* open reading was subcloned into pcDNA3.1D/V5-His-TOPO vector which tagged with V5 with pcDNA 3.1 directional TOPO Expression Kit (Invitrogen, Carlsbad, CA). The *CASK* gene was subcloned into pcDNA3.1/N-terminal-GFP-TOPO vector which tagged with GFP with GFP Fusion TOPO TA Expression Kit (Invitrogen, Carlsbad, CA).

Neuronal Cell Culture and Transfection

HT22 cells, a mouse hippocampal cell line, were maintained in DMEM supplemented with 10% fetal calf serum (Atlanta Biologicals, Norcross, GA) and penicillin/streptomycin at 37°C and 5% CO_2. HEK293H cells, generated by transformation of human embryonic kidney cell cultures, were maintained in the similar condition of HT22 cells. PC12 cell, a cancer cell line derived from a pheochromocytoma of the rat adrenal medulla, were maintained in DMEM supplemented with 15% horse serum 3% FBS, L-glutamine, and penicillin/streptomycin at 37°C and 5% CO_2. Cells were transfected with lipofectamine 2000 (Invitrogen, Carlsbad, CA) with conditions recommended by the supplier. During transfection, cells were maintained in serum- and antibiotic-free medium. After 4 hr of exposure to DNA-lipofectamine mixture, cells were fed with medium containing FBS.

Antibodies and Indirect Immunofluorescence Staining

Cells grown on glass coverslips were fixed and permeabilized with 4% paraformaldehyde (Sigma) and 0.1% Triton X-100 (ICN Biomedicals) in PBS. Fixed cells were blocked in blocking buffer (2% horse serum and 0.4% BSA in PBS) for 30 min. Cells were then incubated with primary antibodies diluted in blocking buffer at appropriate concentrations for 1 hr. The primary antibodies were added simultaneously for the double staining. The mouse anti-V5 antibody and the rabbit anti-GFP antibody were used at a 1:400 and 1:800 dilution, respectively. Subsequent antibody detection was carried out with Rhodamine-conjugated anti-mouse IgG and FITC-conjugated anti-rabbit IgG. Nuclear staining was performed with Sytox Orange (Molecular Probes) staining 5 min. Slides were then viewed under the confocal microscope Zeiss LSM510. The emission filters used for Rhodamine -conjugated and FITC-conjugated fluorescence were 594 nm and 488 nm, respectively.

Coimmunoprecipitation and Western Blot Analysis

HEK293H cells grown in 60 mm diameter tissue-culture plates were transiently transfected with 3 μg of V5-tagged KIRREL3 expression plasmid and/or 3 μg of GFP-tagged CASK expression plasmid with Lipofectamine 2000 (Life Technologies, Inc.) under conditions specified by the supplier. 24 hr after transfection, cells were washed with 1× ice-cold PBS and incubated with 1% NP-40 lysis buffer (1% NP-40; 150 mM NaCl; 50 mM Tris [pH 8.0]) plus protease inhibitor cocktail (Sigma) for at least 10 min on ice. Protein extracts were then collected by 10 min centrifuge at 10,000 × g at 4°C. Cleared supernatant were quantified by Bradford. 500 μg of protein from each experimental group were incubated with 1 μg anti-V5 antibody (anti-rabbit, Sigma) on a spinning rotator at 4°C over night. Magnetic beads conjugated with anti-rabbit antibody (Pierce Inc.) were coated with 1% BSA in 1% NP40 lysis buffer with protease inhibitor cocktail by incubation together at room temperature for 1 hr. The beads were added to the lysate-antibody mixture and incubated on the rotator at 4°C for 2 hr. The immunoprecipitation reaction was washed six times with 1% NP40 lysis buffer with protease inhibitor cocktail for 10 min each at room temperature. Bound protein was eluted with 40 μl 1× sodium dodecyl sulfate (SDS) sample buffer and, after SDS-PAGE, subjected to western blot analysis to detect GFP-tagged protein. Primary antibodies used were the rabbit anti-GFP antibody (Roche) at 1:2000, the mouse anti-V5 antibody (Invitrogen, Carlsbad, CA) at 1:5000. Immunoreactive bands were detected by SuperSignal West Dura (Pierce Inc.) with standard X-ray film (Kodak, Rochester, NY).

Results

Truncation of Two Genes, *CDH15* and *KIRREL3*, by the Translocation Breakpoints in a Patient with ID

To identify potential candidate autosomal genes for ID, we analyzed a 56-year-old female patient (CMS3377) with severe ID who had an apparently balanced translocation t(11;16)(q24.2;q24). Whole-genome array-CGH analysis with a Human Mapping 250K Nsp Array revealed no obvious additional chromosomal imbalance in the patient. We hypothesized that the ID phenotype in the patient was likely resulting from either haploinsufficiency or gain of

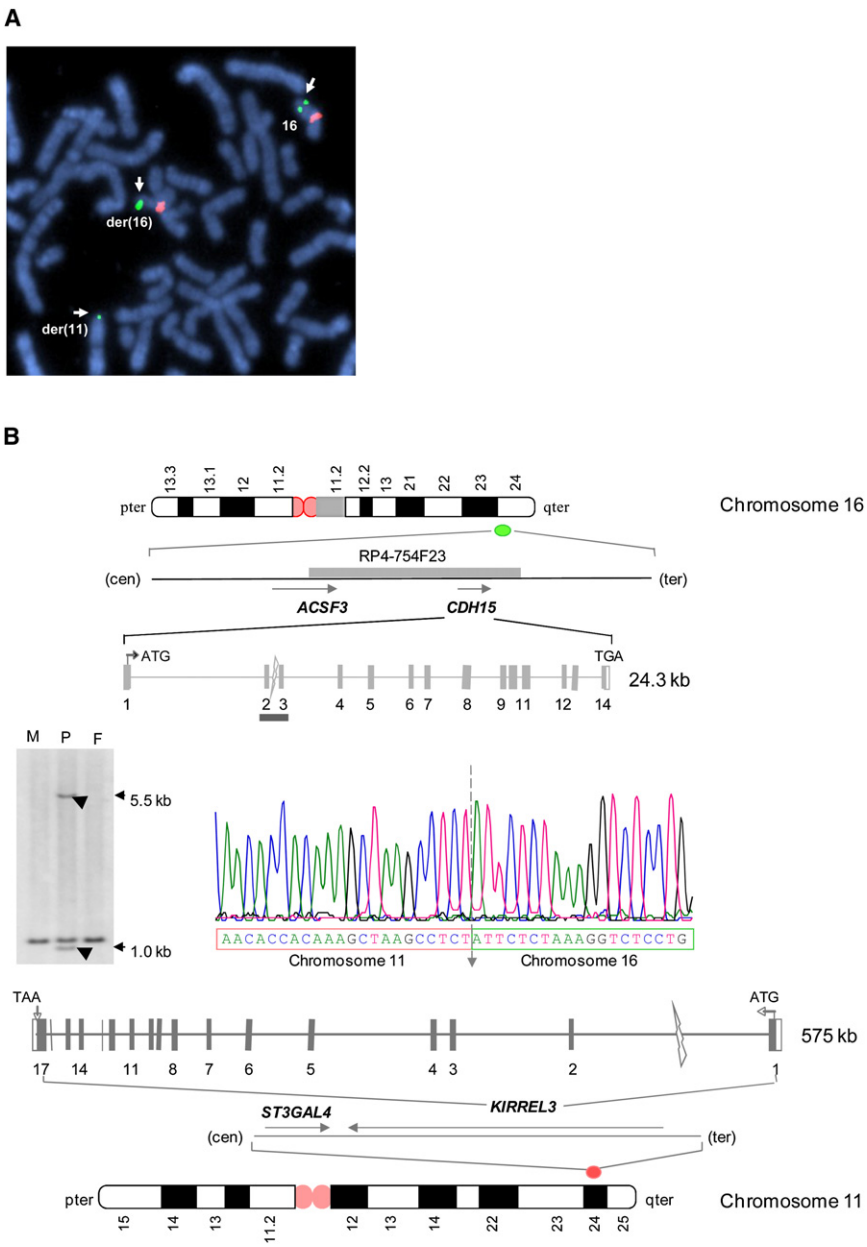

Figure 1. Cloning of the t(11;16) Translocation Breakpoints and Identification of the Candidate ID Genes

(A) Metaphase spread from the female patient with the t(11;16) translocation showing FISH signals obtained with PAC clone RP4-754F23 (green), with a chromosome 16 centromere-specific alphoid sequence probe (red). The hybridization signals (white arrowheads) on both der(16) and der(11) chromosomes indicate that this PAC clone spans the 16q breakpoint.

(B) Genes residing in clone RP4-754F23 are shown. Hybridization of a 1.2 kb probe containing *CDH15* exon 2, intron 2, and exon 3 to a Southern blot containing Pst1 restricted DNA from the patient (P) and from a control male (M) and a control female (F). Novel aberrant restriction fragments (1.0 kb, 5.5 kb) corresponding to the two junction fragments were identified in DNA from the patient (arrowheads). Inverse PCR cloning of the 1.0 kb junction fragment and subsequent sequencing identified the chromosome 11 sequence at the t(11;16) translocation. The chromosome 11 breakpoint junction sequence was mapped in intron 1 of the *KIRREL3* gene.

function of a gene or genes present at or near the breakpoints in 11q and 16q.

By using fluorescence in situ hybridization (FISH), we localized the 16q breakpoint to within the P1-artificial clone (PAC) RP4-754F23 (Figures 1A and 1B). Sequence analysis of the corresponding genomic region revealed that the clone RP4-754F23 contains one known gene, cadherin 15 (*CDH15*),[25] and part of a gene, acyl-CoA synthetase family member 3 (*ACSF3*) (Figure 1B).

The *CDH15* gene has 14 exons spanning about 24.3 kb of genomic DNA. One of the four overlapping probes encompassing the open reading frame of the *CDH15* gene detected a novel fragment in Southern analysis of the patient's DNA digested with EcoR1, Pst1, or Xba1 (data not shown). By using a genomic probe, we fine mapped the 16q24 translocation breakpoint to the second intron of *CDH15* and detected two novel Pst1 DNA fragments (1.0 kb and 5.5 kb) corresponding to two breakpoint junctions (Figure 1B). We cloned the 1.0 kb junction fragment and sequence analysis revealed that it contains the sequence corresponding to intron 2 of *CDH15* as well as sequence from chromosome 11q24 (Figure 1B). The chromosome 11 breakpoint junction sequence mapped to intron 1 of a large gene, *KIRREL3* (*KIAA1867*), originally isolated from a fetal brain cDNA library.[26] The *KIRREL3* gene has 17 exons spanning a genomic region of approximately 575 kb. We further confirmed the sequence of both translocation breakpoint regions by using primers that specifically amplified products from the derivative chromosomes but not from the normal chromosomes (Figure S1). A single base-pair deletion was identified at the 16q24 breakpoint (Figure 1B and data not shown). Extensive FISH analysis detected no additional genomic rearrangements over a large genomic interval (approximately 10 Mb) in the vicinity of the 16q or the 11q breakpoints (see above).

Consistent with disruption of one chromosomal copy, expression of *CDH15* and *KIRREL3* was 38%–45% lower in patient CMS3377 (data not shown) but not in two control individuals. We also analyzed expression of *ST3GAL4*,

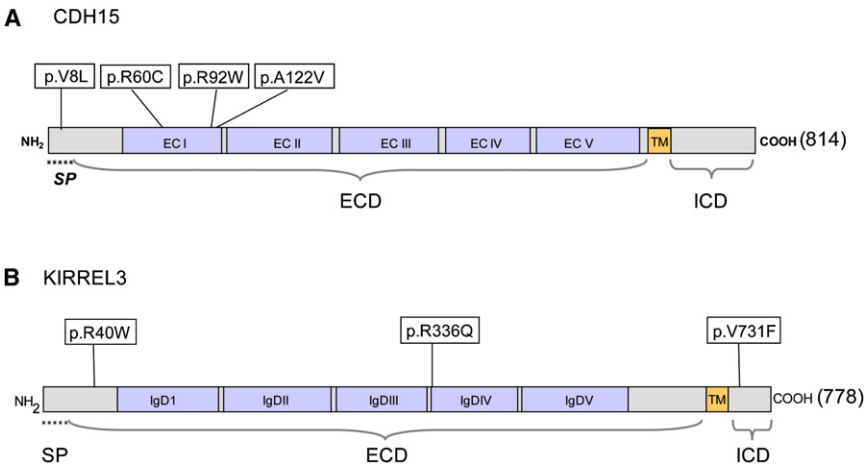

Figure 2. Alterations of CDH15 and KIRREL3

(A) An schematic representation of the CDH15 protein is shown, illustrating the four predicted variations (p.V8L, p.R60C, p.R29W, and p.A122V) found in the ID population; the five extracellular cadherin ectodomain repeats (EC) are boxed. A signal peptide (SP) that extends from amino acid 1 to 21 is also indicated. ECD, extracellular domain; TM, transmembrane domain; ICD, cytoplasmic domain.

(B) Schematic representation of the domains contained in KIRREL3 illustrating the three variations (p.R40W, p.R336Q, and p.V731F) found in the ID population. Positions of the five immunoglobulin domains (Ig) are indicated. A signal peptide (SP) extends from amino acids 1 to 17. The last four amino acids of the KIRREL3 protein constitute a *PDZ* (PSD-95, Dlg, and Zo-1) binding domain. The unclassified alterations found in this study and the alterations identified in the 5′- and 3′-untranslated and intronic regions are not indicated.

a gene mapping centromeric to *KIRREL3* at 11q24 and the *ACSF3* gene mapping centromeric to the *CDH15* at 16q24 (Figure 1B). Expression of *ST3GAL4* and *ACSF3* was identical in the patient and in two controls, ruling out a long-range position effect of the breakpoints.

Expression of the *CDH15* and *KIRREL3* Genes in Brain

Expression of *CDH15* has been shown to be predominantly located in skeletal muscle and human brain.[25] To monitor the expression pattern in human brain regions, we analyzed a northern blot containing RNAs from the different regions of the adult human brain by using a *CDH15* probe. Predominant expression of a transcript of approximately 2.9 kb and faint expression of three larger transcripts (approximately 3.8, 6.9, and 8.0 kb) were detected in whole brain and cerebellum (Figure S2). Other brain sections including occipital lobe, thalamus, and hippocampus showed very faint or no detectable expression.

Northern analysis of fetal and adult human tissues with the *KIRREL3* cDNA as a hybridization probe detected a single transcript of approximately 4.4 kb, exclusively expressed in human fetal and adult brain (Figures S3A and S3B), with undetectable expression in all other tissues tested. The 4.4 kb transcript was expressed with variable levels of expression in all brain regions studied (Figures S3C and S3D). An identical 4.4 kb transcript was also detected in RNAs from 11, 15, and 17 days postcoitum mouse embryos (Figure S3D).

Missense Variants in the *CDH15* and *KIRREL3* Genes in Patients with ID

Molecular cytogenetic and expression data revealed a direct disruption of *CDH15* and *KIRREL3* genes and suggested a potential role for these genes in expression of cognitive dysfunction. Because we had no karyotype information from the deceased parents of the patient, we sought to screen the unrelated cohort of ID patients and controls to investigate whether the alterations in these genes influenced the ID phenotype. We began by sequencing both copies of the *CDH15* and *KIRREL3* genes in the patient with the translocation. No alterations were identified, indicating that the t(11;16) translocation does not unmask a recessive mutation in either gene.

Subsequently we screened for mutations of these two genes in a large cohort of 647 unrelated patients with ID of unknown etiology, via incorporation PCR SSCP[24] combined with direct sequencing. We identified seven nonsynonymous rare variants. These variations were absent in 800 control individuals and more than 600 unrelated patients with ID.

We identified four heterozygous nonsynonymous variants in CDH15 (c.22G → C, p.V8L; c.178C → T, p.R60C; c.274C → T, p.R92W; c.365C → T, p.A122V), each in a single female patient with mild to severe ID. (Figure 2A; Figure S4 and Table S3). The p.R92W variation was identified in a female with mild ID. The patient transmitted her defective allele to her son who also has learning and memory difficulties (Figure S4B). An additional female patient with mild ID inherited the p.A122V variant from her father who was described by family members as having normal cognitive function but had no formal clinical evaluation (Figure S4C). All four residues involved in variations are in the functionally critical regions of CDH15: residue V8 is in the signal peptide region (Figure 2A) and residues R60, R92, and A122 are within the ectodomain 1 (EC1) of CDH15 and are highly conserved among vertebrates and are specifically conserved in mammals (Figure 2A; Table S2A). The functional significance of residue V8 is not clear because it is not conserved in rodents.

Screening of KIRREL3 revealed three heterozygous nonsynonymous variations (c.118C → T, p.R40W; c.1007G → A, p.R336Q; c.2191G → T, p.V731F) in unrelated patients

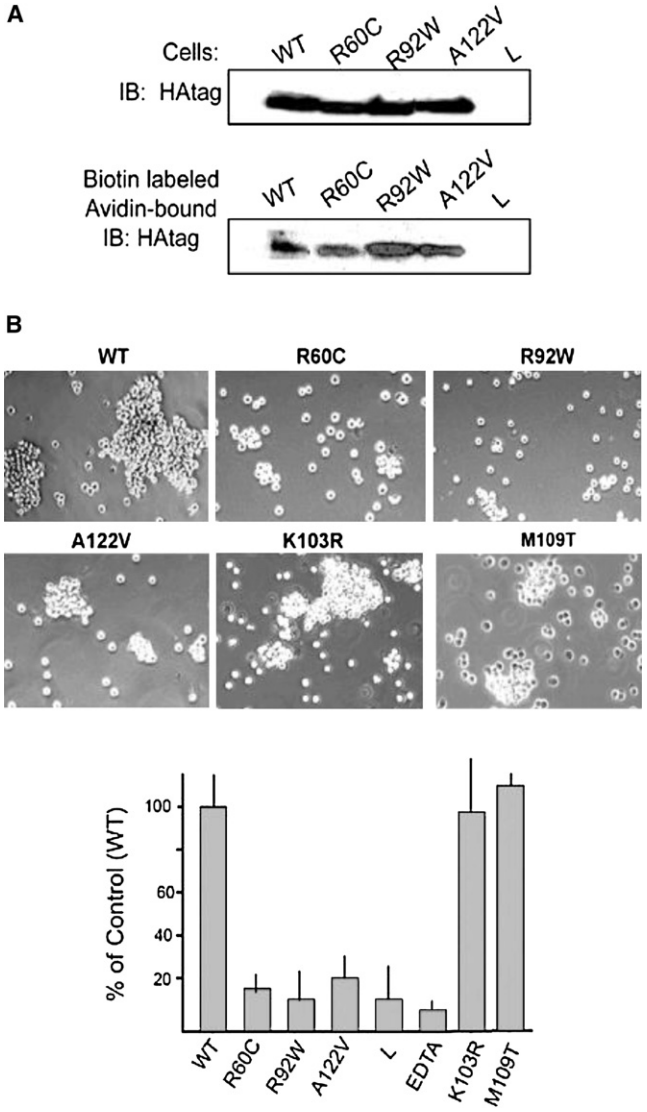

Figure 3. Expression and Adhesion Function of Wild-Type and Mutant Human CDH15 in Mouse L Cells

(A) Western blot analysis of L cells expressing wild-type CDH15 or CDH15 carrying the indicated point variations show similar levels of CDH15 expression (top). Expression at the cell surface is also comparable in all cell types, as shown by biotinylation of cell-surface proteins followed by incubation with avidin beads and western blotting with HA antibody (bottom). WT, L cells expressing wild-type CDH15; L, parental L cells.

(B) L cells expressing CDH15 carrying the missense variations found in ID patients lose the ability to form Ca^{2+}-dependent aggregates. Two control missense variations made in the same EC1 domain, p.K103R and p.M109T, behave like wild-type L cells. Images of aggregates formed at 3 hr (top) and quantification of aggregation measured as the ratio between aggregates greater than 4 cells and single cells after 3 hr in culture (bottom). Both the visual images and the numerical data reveal loss of Ca^{2+}-dependent cell-cell adhesion. EDTA, L cells expressing wild-type CDH15 cultured in the presence of 5 mM EDTA.

with ID (Figure 2B; Figure S5 and Table S3). R40W was present in a female patient with severe ID. The p.R336Q variation was identified in one male and two unrelated female patients with mild to severe ID, and a p.V731F variation was observed in a female patient with mild ID. The residues at all three variations are highly conserved in mammals (Table S2B). Residue R336 is also conserved in a *C. elegans* ortholog, synaptogenesis abnormal protein 1 (SYG-1)[27] (Table S2B).

The Missense Variations Identified in Patients with ID Affect the Cell-Adhesion Properties of CDH15

The most distal cadherin ectodomain, EC1, is considered functionally important and provides the primary adhesive interface for type I and II cadherins (Figure 2A).[28] We examined whether the three amino acid variations in EC1 (p.R60C, p.R92W, and p.A122V) of CDH15 interfere with cell-cell adhesion function. All three base substitutions responsible for the amino acid changes were recreated in the human cDNA clone by site-directed mutagenesis and transfected into mouse L-cells, which lack cadherins. Cell lines expressing either the wild-type or one of the three mutated cDNA clones were assayed for cell-cell adhesion and cell-surface expression (Figure 3). The three mutants and the wild-type cell lines expressed approximately equal amounts of cadherin at the cell surface (Figure 3A), yet cell-cell adhesion among cells derived from each of the three mutated clones was decreased by greater than 80% (Figure 3B). In fact, the clusters that do form among the cell lines containing the mutated clones were indistinguishable from clusters formed by L-cells lacking any cadherins (Figure 3B and data not shown). In contrast, the human protein carrying missense alterations in nonconserved residues in the rodents in the EC1 domain (p.K103R and p.M109T) had no effect on cell-cell adhesion (Figure 3B).

Interaction of *KIRREL3* with the Synaptic Scaffolding Protein CASK

KIRREL3 gene function is largely unknown and therefore we were not able to examine the functional consequences of the *KIRREL3* gene alterations identified in patients with ID. However, these alterations were predicted to be deleterious by at least more than one bioinformatics prediction tools (PolyPhen, PMUT, SIFT). Therefore we attempted to examine a likely function of KIRREL3 in neuronal cells. A role for mouse Kirrel3 in synaptogenesis was suggested based on its temporal and spatial expression in developing and adult mouse brain and its colocalization and interaction with the synaptic scaffolding protein Cask.[21] Furthermore, CASK gene defects have been found recently in patients with ID.[18–20] We hypothesized that in neuronal cells, human KIRREL3 and CASK may work via the same signal transduction pathway.

To examine whether human KIRREL3 and CASK are associated in neuronal cells, we cotransfected HEK293H cells and HT22 cells with KIRREL3-V5 and GFP-CASK constructs and confirmed translation of the correct KIRREL3-V5 and

GFP-CASK fusion proteins by western blot analysis. We assayed for the presence of CASK in immunoprecipitates of KIRREL3 (Figure 4D). Results from both cell lines were consistent: in cells overexpressing CASK and KIRREL3, GFP-CASK is precipitated by the KIRREL3-V5 but not by the equally tagged control protein (LaZ-V5). CASK-specific signal was not detected in control cells expressing only LacZ-V5 or GFP-CASK. Subsequently, we also confirmed endogenous expression of CASK in these cells and confirmed interaction of the endogenous CASK with KIRREL3-V5 via a CASK-specific antibody (Figure 4E).

We examined whether KIRREL3 and CASK are also colocalized in neuronal cell. First to examine the localization of KIRREL3 protein in neurons, PC12 cells were transiently transfected with a KIRREL3-V5 fusion construct and then stained with V5 antibody. Confocal microscopy showed KIRREL3-positive staining in a ring shape implying its expression on cell membrane (Figure 4A). Some likely cytoplasmic signal was also noted.

To study colocalization of KIRREL3 and CASK, we cotransfected PC12 cells with KIRREL3-V5 and GFP-CASK constructs. Immunostaining reveals the colocalization of these two proteins (Figure 4B). We also examined the colocalization of both proteins in HT22 cells (Figure 4C). Again, CASK expression was found to overlap with the expression of KIRREL3. CASK is primarily a cytoplasmic protein that interacts with several membrane proteins[29] and as expected, CASK signals were also noted in areas where KIRREL3 was not expressed (Figures 4B and 4C).

Discussion

Balanced de novo chromosomal rearrangements are associated with abnormal phenotypes in about 6% of cases[30] and are often found to affect the gene or genes at or near the breakpoints. Such translocations in patients with ID have been proven to be valuable resource in the search for genes causally related to disease. Our study identifies two genes, *CDH15* and *KIRREL3*, physically disrupted by the translocation breakpoints in a female patient with severe ID. Both genes are expressed in the brain, and a putative role for these two genes in brain function critical for learning and memory has been predicted. We also identified several nonsynonymous sequence variations in each of these two genes in unrelated patients with ID. The variations were absent in 800 control individuals and 600 individuals with ID. In one case, a *CDH15* variation was also identified in a mother and son, both with learning and memory problems. We hypothesized that these rare variants are likely to be functionally important and may influence gene function in the brain that is critical for learning and memory. To support this, our in vivo functional studies provided evidence that only CDH15 variations, identified in patients with ID, adversely alter its ability to mediate cell-cell adhesion. Unfortunately, we have no comparable evidence for the *KIRREL3* gene alterations. Nonetheless, the KIRREL3 alterations identified in patients with ID were predicted to be deleterious and found to be in conserved residues. Thus we examined a potential role for KIRREL3 in neuronal cells and showed that KIRREL3 interacts and colocalizes with the synaptic scaffolding protein CASK, also recently implicated in ID.

Individuals affected with ID usually do not have children and thus a large number of mutations causing autosomal-dominant ID are de novo including chromosomal rearrangements associated with ID. Although the karyotypes of the parents are not known, we strongly suspect that the translocation is de novo in the patient and speculate that the disruption of both genes in the patient with the t(11;16) translocation may have contributed to the severity of ID. This patient also has finger anomalies, including syndactyly, where none of the patients carrying variants in either gene exhibits such anomalies. It is likely that the anomalies may be due to an additional factor or modifying gene.

Finding several rare nonsynonymous sequence variations in each of these two genes in unrelated patients with ID suggests that alterations in either gene are likely to affect brain function and may contribute to mild to severe ID. However, some of these rare variants might contribute to disease risk, and additional factors may be required to complete expression of ID phenotype. Such a possibility has recently been noted in studies involving two genes, Neurexin1 (*NRXN1*) (MIM 600565) and Contactin associated protein-like 2 (*CNTNAP2*) (MIM 604569), suggesting the contribution of conserved rare variants to disease risk.[13,14] Moreover, the significance of rare missense variations in patients remains critical considering several SNPs in other genes have been found to be functionally important.[31]

The first gene, *CDH15*, encodes a protein of 814 amino acid residues[25] (Figure 2A). It belongs to the type I classic cadherin superfamily group, all of which are single-pass transmembrane molecules with five extracellular (EC) repeats that mediate calcium-dependent homophilic, cell-cell adhesion.[25,32] Additionally, all members of this group have a highly conserved cytoplasmic domain that interacts with β-catenin, which in turn interacts with α-catenin regulating cytoskeletal function at adherens junctions[33] (Figure 5). The four identified missense alterations in CDH15 are all clustered in the N-terminal region. Residue R60 is highly conserved in M, N, and R cadherins (Table S2A), all primarily neural and thus may be critical for neural function in general. Residue R92 is specific to mammalian cadherin 15 (M-cadherins) and thus may play a specific role in CDH15 function. *CDH15* is also expressed in skeletal muscle. However, none of the patients with *CDH15* variations have a skeletal muscle disorder. In one case, we noticed that a 46-year-old patient with the p.R60C CDH15 variation had her finger reported to extend only to neutral and her elbow did not extend to neutral, and in a second case, a 44-year-old patient with the p.A122V variation reportedly has facial muscle hypotonia and short distal phalanges.

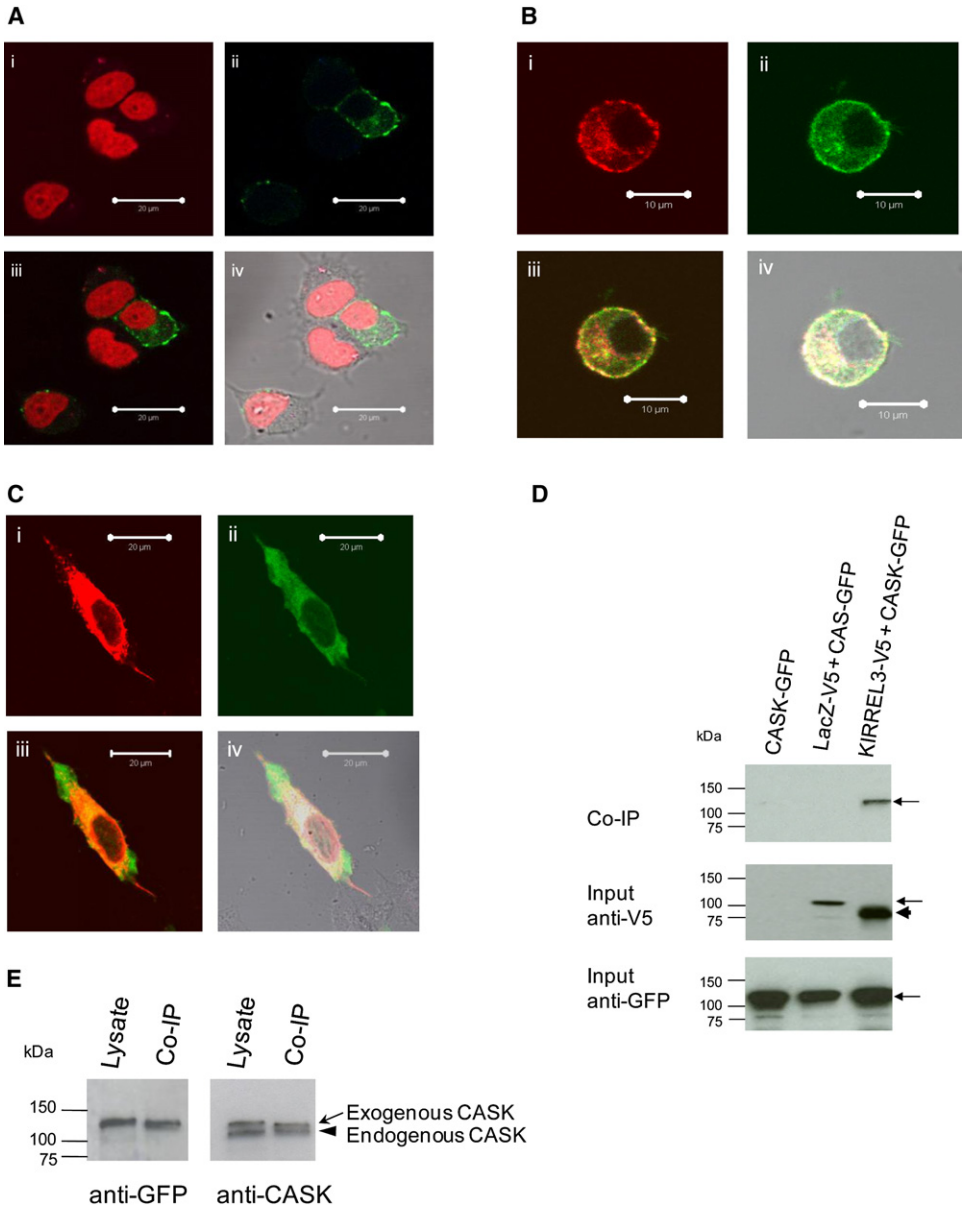

Figure 4. Expression of Wild-Type KIRREL3 and Its Interaction with CASK

(A) KIRREL3-V5-overexpressing PC12 cells showing localization of KIRREL3 (green) on cell membrane (ii). Nuclei were stained with sytox (red) (i). Staining of KIRREL3 and nucleus were shown simultaneously in (iii). Fluorescence staining was merged with differential interference contrast (DIC) image to illustrate the cells' shape (iv).

(B and C) KIRREL3-V5 and GFP-CASK co-overexpressing PC12 cells (B) and HT22 cells (C), expression of KIRREL3 (red) (i) and CASK (green) (ii) are shown. The colocalization was shown as yellow/orange within the region of cell membrane and possibly cytoplasma (iii). DIC image was demonstrated together with the double staining (iv). For each experiment, at least 60 transfected cells were examined.

(D) Interaction between KIRREL3 and CASK. Lysates prepared from KIRREL3-V5- and GFP-CASK-overexpressing HEK293H cells were incubated with V5 antibody and subsequently precipitated with magnetic beads. Bound CASK was detected by western blot analysis (top) with the rabbit GFP antibody. KIRREL3-V5 but not LacZ-V5 or CASK itself immobilizes CASK (arrow), suggesting that KIRREL3 and CASK interact in cells. To examine the expression of KIRREL3, the same blot was reprobed with V5 antibody (middle). LacZ-V5 (arrow) and KIRREL3-V5 (arrowhead) were detected as indicated in the respective lanes. Comparable amounts of CASK protein were loaded in each lane (bottom). The co-IP results were verified in three separate experiments.

(E) GFP-CASK- and KIRREL3-V5-overexpressing HEK293H cells protein lysate was coimmunoprecipitated with V5 antibody. Immunoblotting with CASK antibody detected endogenous CASK in KIRREL3-V5 immunoprecipitate suggesting endogenous expression of CASK and its interaction with KIRREL3-V5.

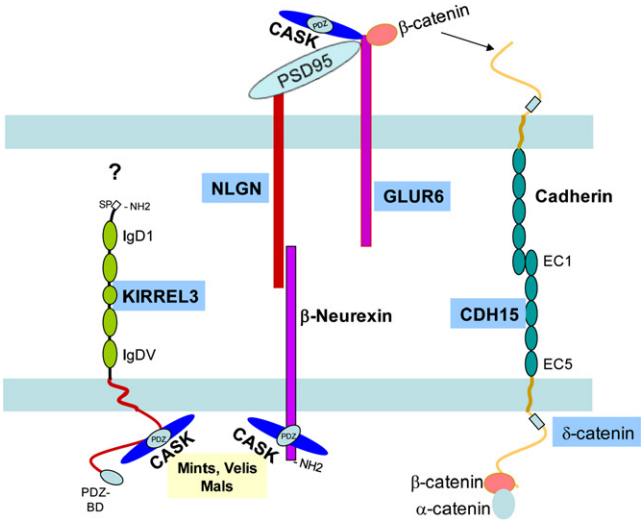

Figure 5. Putative Signaling System Likely to Influence Human Cognition Involving Cadherin, KIRREL3, and CASK
Variations identified in CDH15 and KIRREL3 are boxed. Previously identified genes with variations in patients with cognitive impairment are shaded in light blue.[10,16,18–20,43–47]

Interestingly, in one patient, a p.R92W variation was transmitted to her son who also has learning and memory difficulties. Residue A122 is in the middle of the critical "HAV" sequence known to be critical for all type 1 classic cadherins and this is important for adhesion in general and differentiates type 1 cadherins from type 2 cadherins. However, the p.A122V variation in the patient (CMS7914) was inherited from the father who reportedly lacks an ID phenotype (Figure S4C). This indicates that the segregation of this variant might show incomplete penetrance and may produce ID only upon interaction with other factors. Nonetheless, our in vivo functional studies showed that the three variations (p.R60C, p.R92W, and p.A122V) in the EC1 domain of CDH15 significantly affect its ability to mediate cell-cell adhesion. Additionally, missense alterations considered to be polymorphisms (p.K103R and p.M109T) in two nonconserved residues in the EC1 domain did not alter cell-adhesion function (Figure 3B). These results support the inference that the residues altered in the ID patients are important for CDH15 function. In the mouse, *Cdh15* gene expression is restricted to the granular layer of the cerebellar cortex in synapses and other intercellular junctions.[34,35] Indeed, a role for cadherins in synaptic plasticity has long been appreciated.[17,36] Recently, defects in two protocadherin genes, *PCDH19* (MIM 300460) and *PCDH10* (MIM 608286), have been shown to be associated with cognitive impairment in humans.[37,38]

The second gene, *KIRREL3,* is a mammalian homolog of the gene *kirre* (kin of irregular chiasm C-roughest) of *Drosophila melanogaster.*[39,40] The *KIRREL3* gene is predicted to encode a type 1a membrane protein of 778 amino acids containing five Ig-like domains in its extracellular portion and a *PDZ* domain-binding motif in its cytoplasmic portion (Figure 2B). Expression of the *KIRREL3* gene was detected exclusively in human fetal and adult brain. Consistent with a vital role in brain development and function, spatiotemporal expression patterns of the mouse gene, mKirre, in developing and adult brain regions, including postnatal hippocampus, suggest a role for mKirre in axonal projections and synapse formation.[41] Finding a KIRREL3-CASK interaction in neuronal cells and colocalization of both proteins in the developing and adult mouse brain[21] suggest that KIRREL3 and CASK may work coordinately (Figure 5). These findings are important because the deletion of *Cask* in mice impairs synaptic function,[22] and defects of the *CASK* gene in humans cause X-linked ID.[18–20] Identification of the extracellular binding partner(s) of KIRREL3 will help to further define the mechanism underlying its physiological function.

Several recent studies suggest that ID might be caused by defects in synapse structure and function. Both the cadherin and immunoglobulin protein superfamilies play critical roles in the developing brain and have been implicated in synapse formation, maintenance, structure, function, and plasticity.[17,36] A schematic diagram of possible interactions involving cadherin, KIRREL3, and CASK is depicted in Figure 5. This scheme is based on recent findings suggesting that genes affecting cognitive function likely participate in a signaling pathway involving CASK,[29] as well as the data presented here. CASK is known to interact with neurexins that in turn bind to the neuroligin/PSD95 complex.[29] Furthermore, a recently identified autosmal-recessive ID protein, GLUR6 (MIM 138244), also interacts with CASK, β-catenin (MIM 116806), and PSD95 (MIM 602887).[10,42] A role for neurexins, neuroligins, and SHANK3 (MIM 606230), a synaptic scaffolder that can also bind to neuroligins, in the cognitive dysfunction associated with autistic spectrum of disorders has been suggested.[43–46] Based on these known interactions, it is tempting to speculate that KIRREL3-CASK-cadherin/catenin all work in a coordinated fashion that affects cognitive function. Of course, additional direct experimental evidence will be required to support this hypothesis.

Altogether, our studies point to a likely contribution of CDH15 and KIRREL3 in learning and memory. Further study in animal models should provide a system to examine how these two proteins contribute to cognitive function in humans and may help further the understanding of the genetic etiology of ID.

Supplemental Data

Supplemental Data include five figures and three tables and can be found with this article online at http://www.ajhg.org/.

Acknowledgments

We wish to express our gratitude to the patients and their families for cooperation. We thank R.C. Rogers, S.A. Skinner, L.H. Seaver,

and K.B. Clarkson for providing clinical details of patients; D. Bealer and C. Skinner for assistance in obtaining patients' samples; T. Moss for help with cell culture; D. Schultz for assistance in sequencing; L. Allen and J. John for technical assistance in mutation screening; J. Collins for assistance in statistical analysis and for discussion; K. Franek and J. Norris for assistance in preparation of expression constructs and confocal microscopy; and C.E. Schwartz and R.E. Stevenson for helpful discussion. This work was supported by a grant from the National Institutes of Child Health and Human Development (R01-HD39331 to A.K.S.) and from the National Eye Institute (R01-EY013363 to J.L. and J.B.). The authors report no conflict of interest.

Received: September 15, 2008
Revised: October 18, 2008
Accepted: October 24, 2008
Published online: November 13, 2008

Web Resources

The URLs for data presented herein are as follows:

Ensembl Genome Browser, http://www.ensemble.org/
HUGO nomenclature committee, http://www.genenames.org/
NCBI Human Genome Browser and Database, http://www.ncbi.nlm.nih.gov/
Online Mendelian Inheritance in Man (OMIM), http://www.ncbi.nlm.nih.gov/Omim/
PMUT, http://mmb.pcb.ub.es/PMut/
PolyPhen, http://genetics.bwh.harvard.edu/pph/
SIFT, http://blocks.fhcrc.org/sift/SIFT_seq_submit2.html
UCSC Human Genome Browser, http://genome.usc.edu/cgi-bin/hgGateway

References

1. American Association on Mental Retardation. (2002). Mental Retardation: Definition, Classification and Systems of Support, Tenth Edition (Washington, DC: American Association on Mental Retardation).
2. Inlow, J.K., and Restifo, L.L. (2004). Molecular and comparative genetics of mental retardation. Genetics *166*, 835–881.
3. Ropers, H.H. (2008). Genetics of intellectual disability. Curr. Opin. Genet. Dev. *18*, 241–250.
4. Chelly, J., Khelfaoui, M., Francis, F., Cherif, B., and Bienvenu, T. (2006). Genetics and pathophysiology of mental retardation. Eur. J. Hum. Genet. *14*, 701–713.
5. Chiurazzi, P., Schwartz, C.E., Gecz, J., and Neri, G. (2008). XLMR genes: Update 2007. Eur. J. Hum. Genet. *16*, 422–434.
6. Basel-Vanagaite, L. (2007). Genetics of autosomal recessive non-syndromic mental retardation: Recent advances. Clin. Genet. *72*, 167–174.
7. Molinari, F., Rio, M., Meskenaite, V., Encha-Razavi, F., Auge, J., Bacq, D., Briault, S., Vekemans, M., Munnich, A., Attie-Bitach, T., et al. (2002). Truncating neurotrypsin mutation in autosomal recessive nonsyndromic mental retardation. Science *298*, 1779–1781.
8. Higgins, J.J., Pucilowska, J., Lombardi, R.Q., and Rooney, J.P. (2004). A mutation in a novel ATP-dependent Lon protease gene in a kindred with mild mental retardation. Neurology *63*, 1927–1931.
9. Basel-Vanagaite, L., Attia, R., Yahav, M., Ferland, R.J., Anteki, L., Walsh, C.A., Olender, T., Straussberg, R., Magal, N., Taub, E., et al. (2006). The CC2D1A, a member of a new gene family with C2 domains, is involved in autosomal recessive nonsyndromic mental retardation. J. Med. Genet. *43*, 203–210.
10. Motazacker, M.M., Rost, B.R., Hucho, T., Garshasbi, M., Kahrizi, K., Ullmann, R., Abedini, S.S., Nieh, S.E., Amini, S.H., Goswami, C., et al. (2007). A defect in the ionotropic glutamate receptor 6 gene (GRIK2) is associated with autosomal recessive mental retardation. Am. J. Hum. Genet. *81*, 792–798.
11. Molinari, F., Foulquier, F., Tarpey, P.S., Morelle, W., Boissel, S., Teague, J., Edkins, S., Futreal, P.A., Stratton, M.R., Turner, G., et al. (2008). Oligosaccharyltransferase-subunit mutations in nonsyndromic mental retardation. Am. J. Hum. Genet. *82*, 1150–1157.
12. Garshasbi, M., Hadavi, V., Habibi, H., Kahrizi, K., Kariminejad, R., Behjati, F., Tzschach, A., Najmabadi, H., Ropers, H.H., and Kuss, A.W. (2008). A defect in the TUSC3 gene is associated with autosomal recessive mental retardation. Am. J. Hum. Genet. *82*, 1158–1164.
13. Bakkaloglu, B., O'Roak, B.J., Louvi, A., Gupta, A.R., Abelson, J.F., Morgan, T.M., Chawarska, K., Klin, A., Ercan-Sencicek, A.G., Stillman, A.A., et al. (2008). Molecular cytogenetic analysis and resequencing of contactin associated protein-like 2 in autism spectrum disorders. Am. J. Hum. Genet. *82*, 165–173.
14. Kim, H.G., Kishikawa, S., Higgins, A.W., Seong, I.S., Donovan, D.J., Shen, Y., Lally, E., Weiss, L.A., Najm, J., Kutsche, K., et al. (2008). Disruption of neurexin 1 associated with autism spectrum disorder. Am. J. Hum. Genet. *82*, 199–207.
15. Arking, D.E., Cutler, D.J., Brune, C.W., Teslovich, T.M., West, K., Ikeda, M., Rea, A., Guy, M., Lin, S., Cook, E.H., et al. (2008). A common genetic variant in the neurexin superfamily member CNTNAP2 increases familial risk of autism. Am. J. Hum. Genet. *82*, 160–164.
16. Laumonnier, F., Cuthbert, P.C., and Grant, S.G. (2007). The role of neuronal complexes in human X-linked brain diseases. Am. J. Hum. Genet. *80*, 205–220.
17. Yamagata, M., Sanes, J.R., and Weiner, J.A. (2003). Synaptic adhesion molecules. Curr. Opin. Cell Biol. *15*, 621–632.
18. Najm, J., Horn, D., Wimplinger, I., Golden, J.A., Chizhikov, V.V., Sudi, J., Christian, S.L., Ullmann, R., Kuechler, A., Haas, C.A., et al. (2008). Mutations of CASK cause an X-linked brain malformation phenotype with microcephaly and hypoplasia of the brainstem and cerebellum. Nat. Genet. *40*, 1065–1067.
19. Froyen, G., Van Esch, H., Bauters, M., Hollanders, K., Frints, S.G., Vermeesch, J.R., Devriendt, K., Fryns, J.P., and Marynen, P. (2007). Detection of genomic copy number changes in patients with idiopathic mental retardation by high-resolution X-array-CGH: important role for increased gene dosage of XLMR genes. Hum. Mutat. *28*, 1034–1042.
20. Piluso, G., D'Amico, F., Saccone, V., Rotundo, L., and Nigro, V. (2007). A missense mutation in CASK gene causes FG syndrome in an Italian GFS family. *13th International Workshop on Fragile X and X-Linked Mental Retardation*. (http://xlmr.interfree.it/home.htm), Abstract P58.
21. Gerke, P., Benzing, T., Hohne, M., Kispert, A., Frotscher, M., Walz, G., and Kretz, O. (2006). Neuronal expression and interaction with the synaptic protein CASK suggest a role for Neph1 and Neph2 in synaptogenesis. J. Comp. Neurol. *498*, 466–475.
22. Atasoy, D., Schoch, S., Ho, A., Nadasy, K.A., Liu, X., Zhang, W., Mukherjee, K., Nosyreva, E.D., Fernandez-Chacon, R., Missler,

M., et al. (2007). Deletion of CASK in mice is leathal and impairs synaptic function. Proc. Natl. Acad. Sci. USA *104*, 2525–2530.
23. Griggs, B.L., Ladd, S., Saul, R.A., DuPont, B.R., and Srivastava, A.K. (2008). Dedicator of cytokinesis 8 is disrupted in two patients with mental retardation and developmental disabilities. Genomics *91*, 195–202.
24. Sossey-Alaoui, K., Lyon, J.A., Jones, L., Abidi, F.E., Hartung, A.J., Hane, B., Schwartz, C.E., Stevenson, R.E., and Srivastava, A.K. (1999). Molecular cloning and characterization of TRPC5 (HTRP5), the human homologue of a mouse brain receptor-activated capacitative Ca2+ entry channel. Genomics *60*, 330–340.
25. Shimoyama, Y., Shibata, T., Kitajima, M., and Hirohashi, S. (1998). Molecular cloning and characterization of a novel human classic cadherin homologous with mouse muscle cadherin. J. Biol. Chem. *273*, 10011–10018.
26. Nagase, T., Nakayama, M., Nakajima, D., Kikuno, R., and Ohara, O. (2001). Prediction of the coding sequences of unidentified human genes. XX. The complete sequences of 100 new cDNA clones from brain which code for large proteins in vitro. DNA Res. *8*, 85–95.
27. Shen, K., and Bargmann, C.I. (2003). The immunoglobulin superfamily protein SYG-1 determines the location of specific synapses in *C. elegans*. Cell *112*, 619–630.
28. Koch, A.W., Manzur, K.L., and Shan, W. (2004). Structure-based models of cadherin-mediated cell adhesion: The evolution continues. Cell. Mol. Life Sci. *61*, 1884–1895.
29. Hsueh, Y.P. (2006). The role of the MAGUK protein CASK in neural development and synaptic function. Curr. Med. Chem. *13*, 1915–1927.
30. Warburton, D. (1991). De novo balanced chromosome rearrangements and extra marker chromosomes identified at prenatal diagnosis: Clinical significance and distribution of breakpoints. Am. J. Hum. Genet. *49*, 995–1013.
31. Sethupathy, P., Borel, C., Gagnebin, M., Grant, G.R., Deutsch, S., Elton, T.S., Hatzigeorgiou, A.G., and Antonarakis, S.E. (2007). Human microRNA-155 on chromosome 21 differentially interacts with its polymorphic target in the AGTR1 3′ untranslated region: A mechanism for functional single-nucleotide polymorphisms related to phenotypes. Am. J. Hum. Genet. *81*, 405–413.
32. Lilien, J., Balsamo, J., Arregui, C., and Xu, G. (2002). Turn-off, drop-out: Functional state switching of cadherins. Dev. Dyn. *224*, 18–29.
33. Yamada, S., Pokutta, S., Drees, F., Weis, W.I., and Nelson, W.J. (2005). Deconstructing the cadherin-catenin-actin complex. Cell *123*, 889–901.
34. Bahjaoui-Bouhaddi, M., Padilla, F., Nicolet, M., Cifuentes-Diaz, C., Fellmann, D., and Mege, R.M. (1997). Localized deposition of M-cadherin in the glomeruli of the granular layer during the postnatal development of mouse cerebellum. J. Comp. Neurol. *378*, 180–195.
35. Rose, O., Grund, C., Reinhardt, S., Starzinski-Powitz, A., and Franke, W.W. (1995). Contactus adherens, a special type of plaque-bearing adhering junction containing M-cadherin, in the granule cell layer of the cerebellar glomerulus. Proc. Natl. Acad. Sci. USA *92*, 6022–6026.
36. Bamji, S.X. (2005). Cadherins: Actin with the cytoskeleton to form synapses. Neuron *47*, 175–178.
37. Dibbens, L.M., Tarpey, P.S., Hynes, K., Bayly, M.A., Scheffer, I.E., Smith, R., Bomar, J., Sutton, E., Vandeleur, L., Shoubridge, C., et al. (2008). X-linked protocadherin 19 mutations cause female-limited epilepsy and cognitive impairment. Nat. Genet. *40*, 776–781.
38. Morrow, E.M., Yoo, S.Y., Flavell, S.W., Kim, T.K., Lin, Y., Hill, R.S., Mukaddes, N.M., Balkhy, S., Gascon, G., Hashmi, A., et al. (2008). Identifying autism loci and genes by tracing recent shared ancestry. Science *321*, 218–223.
39. Ueno, H., Sakita-Ishikawa, M., Morikawa, Y., Nakano, T., Kitamura, T., and Saito, M. (2003). A stromal cell-derived membrane protein that supports hematopoietic stem cells. Nat. Immunol. *4*, 457–463.
40. Ramos, R.G., Igloi, G.L., Lichte, B., Baumann, U., Maier, D., Schneider, T., Brandstatter, J.H., Frohlich, A., and Fischbach, K.F. (1993). The irregular chiasm C-roughest locus of *Drosophila*, which affects axonal projections and programmed cell death, encodes a novel immunoglobulin-like protein. Genes Dev. *7*, 2533–2547.
41. Tamura, S., Morikawa, Y., Hisaoka, T., Ueno, H., Kitamura, T., and Senba, E. (2005). Expression of mKirre, a mammalian homolog of *Drosophila* Kirre, in the developing and adult mouse brain. Neuroscience *133*, 615–624.
42. Coussen, F., Normand, E., Marchal, C., Costet, P., Choquet, D., Lambert, M., Mège, R.M., and Mulle, C. (2002). Recruitment of the kainate receptor subunit glutamate receptor 6 by cadherin/catenin complexes. J. Neurosci. *22*, 6426–6436.
43. Autism Genome Project Consortium. (2007). Mapping autism risk loci using genetic linkage and chromosomal rearrangements. Nat. Genet. *39*, 319–328.
44. Durand, C.M., Betancur, C., Boeckers, T.M., Bockmann, J., Chaste, P., Fauchereau, F., Nygren, G., Rastam, M., Gillberg, I.C., Anckarsater, H., et al. (2007). Mutations in the gene encoding the synaptic scaffolding protein SHANK3 are associated with autism spectrum disorders. Nat. Genet. *39*, 25–27.
45. Jamain, S., Quach, H., Betancur, C., Rastam, M., Colineaux, C., Gillberg, I.C., Soderstrom, H., Giros, B., Leboyer, M., Gillberg, C., et al. (2003). Mutations of the X-linked genes encoding neuroligins NLGN3 and NLGN4 are associated with autism. Nat. Genet. *34*, 27–29.
46. Laumonnier, F., Bonnet-Brilhault, F., Gomot, M., Blanc, R., David, A., Moizard, M.P., Raynaud, M., Ronce, N., Lemonnier, E., Calvas, P., et al. (2004). X-linked mental retardation and autism are associated with a mutation in the NLGN4 gene, a member of the neuroligin family. Am. J. Hum. Genet. *74*, 552–557.
47. Israely, I., Costa, R.M., Xie, C.W., Silva, A.J., Kosik, K.S., and Liu, X. (2004). Deletion of the neuron-specific protein delta-catenin leads to severe cognitive and synaptic dysfunction. Curr. Biol. *14*, 1657–1663.